Cell, Volume *130*

Supplemental Data

An Intracellular Serpin Regulates Necrosis by Inhibiting the Induction and Sequelae of Lysosomal Injury

Cliff J. Luke, Stephen C. Pak, Yuko S. Askew, Terra L. Naviglia, David J. Askew, Shila M. Nobar, Anne C. Vetica, Olivia S. Long, Simon C. Watkins, Donna B. Stolz, Robert J. Barstead, Gary L. Moulder, Dieter Brömme, and Gary A. Silverman

Supplemental Experimental Procedures

Plasmid Construction and Transgenic Animals

For expression constructs, the *srp-6* promoter (P) region (2.8 kbp upstream from the putative start codon) through exon 2 was amplified from N2 genomic DNA. The PCR product was cloned into pPD95.77 in frame with GFP. The p$P_{srp\text{-}6}$*::GFP* translational fusion construct was co-injected with pRF4 (contains *rol-6(su1006)*) into the gonads of gravid adult N2 animals and roller progeny were isolated. GFP localization was visualized using a Zeiss Axioskop II Mot with Normarski (DIC) optics using excitation and emission wavelengths of 492 nm and 530 nm, respectively.

For srp-6 rescue constructs, the *srp-6* promoter region through the 3'-UTR (4.2 kbp) was amplified from N2 genomic DNA. The PCR product was ligated into pPD95.03 to yield p*srp-6*. For intestinal cell specific rescue constructs, the *nhx-2* promoter (generously provided by Keith Nehrke) was amplified from N2 genomic DNA and cloned into pPD95.85 (Nehrke, 2003). The genomic *srp-6* genomic DNA, including all six exons from the putative start site to the terminal codon, were cloned 3' to the *nhx-2* promoter to yield p$P_{nhx\text{-}2}$*srp-6*. To generate RSL variants, p*srp-6* or p$P_{nhx\text{-}2}$*srp-6* was mutated at the canonical P14 and P2-1 positions using a site-directed mutagenesis kit (Stratagene) to yield p*srp-6(T327R)*, p$P_{nhx\text{-}2}$*srp-6(T327R)* and p*srp-6(L339A;T340A)*, respectively. Each of the five different rescue constructs was co-injected with the p$P_{nhx\text{-}2}$*::GFP* plasmid into *srp-6(ok319)* animals. The GFP positive progeny were used to establish several separate lines for each construct. The lines were designated VK247 (*srp-6(ok319);vkEx247[srp-6(L339A;T340A);*$P_{nhx\text{-}2}$*::GFP]*), VK248 (*srp-6(ok319);vkEx248[srp-6(T327R);*$P_{nhx\text{-}2}$*::GFP]*), VK249 (*srp-6(ok319);vkEx249[srp-6(+);*$P_{nhx\text{-}2}$*::GFP]*), VK611 (*srp-6(ok319);vkEx611[*$P_{nhx\text{-}2}$*srp-6;*$P_{nhx\text{-}2}$*::GFP]*) and VK618 (*srp-6(ok319);vkEx618[*$P_{nhx\text{-}2}$*srp-6(T327R);*$P_{nhx\text{-}2}$*::GFP]*).

For *mec-4(d)* expression constructs, the *mec-4(d)* gene was amplified from a plasmid containing the HindIII genomic fragment from *mec-4(u231)* (generously provided by Monica Driscoll) (Driscoll and Chalfie, 1991). The PCR product, containing the start and termination codons of the *mec-4(d)* gene, was ligated 3' to the *hsp-16* promoter in pPD49.83 to yield p$P_{hsp\text{-}16}$*mec-4(d)*. This construct was then co-injected with the p$P_{nhx\text{-}2}$*::GFP* plasmid into *srp-6(+)* and *srp-6(ok319)* animals. GFP positive progeny were selected and yielded several independent lines

designated VK594 (*srp-6(+);vkEx594[P_{hsp-16}mec-4(d);P_{nhx-2}::GFP]*) and VK599 (*srp-6(ok319);vkEx599[P_{hsp-16}mec-4(d);P_{nhx-2}::GFP]*).

Drug Treatments

For all drug treatments, the compound was incubated with either *srp-6(+)* or *srp-6(ok319)* animals at the indicated concentration in M9 at room temperature. Worms were washed 3 times with M9 before being assayed. The peptidase inhibitors E-64d ((2S,3S)-*trans*-Epoxysuccinyl-L-leucylamido-3-methylbutane ethyl ester; Sigma), Ac-DEVD-CHO (acetyl-Asp-Glu-Val-Asp-aldehyde; Calbiochem) and Ac-YVAD-CHO (acetyl-Tyr-Val-Ala-Asp-aldehyde; Calbiochem) were incubated for 1 h at final concentrations of 10 μM, 100 μM and 100 μM, respectively. The calcium chelators, EGTA-AM (ethyleneglycol-*bis*-(β-aminoethyl)-N,N,N',N'-tetraacetoxymethyl ester) and BAPTA-AM (1,2-*bis*-(o-aminophenyl)-ethyleneglycol-N,N,N',N'-tetraacetic acid, tetraacetoxymethyl ester) (Molecular Probes) were incubated for 2 h at a final concentration of 100 μM. Thapsigargin (Calbiochem) was incubated for 1 h at a final concentration of 100 μM.

Imaging Studies

For initial calcium imaging, young adult *srp-6(+)* or *srp-6(ok319)* animals were labelled with for 1 h with 100 μM Fluo-4 AM (Molecular Probes) and 1% Pluronic F127 (Molecular Probes) dissolved in M9 (Espelt et al., 2005). Approximately 10 animals per time point were subjected to hypotonic shock at 25 ºC or 10 ºC, removed at the indicated time and visualized using a Zeiss Axioskop II Mot with Normarski (DIC) optics. For consistency, the region of interest was demarcated as the apical cytoplasm of the proximal intestine located just distal to the pharyngeal-intestinal valve. The excitation and emission wavelengths were 492 nm and 530 nm, respectively. Relative fluorescence (F_1/F_0) was calculated using OpenLab 3.1.3 (Improvision), where F_1 was the fluorescence at the indicated time point and F_0 was the fluorescence at time 0. For calcium fluxes in the presence of E-64d, *srp-6(+)* or *srp-6(ok319)* animals were incubated with Fluo-4 AM and Pluronic F127 for 1 h as above, and then treated with 10 μM E-64d (Sigma) for 30 min at 25ºC prior to hypotonic shock.

To visualize lysosome-like gut granules, L4 *srp-6(+)* or *srp-6(ok319)* animals were labelled with 10,000 MW dextran-TMR (Molecular Probes) at a final concentration of 10 mg/ml as described (Hermann et al., 2005), except that the animals were incubated for 12 h in M9 buffer. Animals were recovered for 4 h on NGM plates seeded with OP50. Animals were exposed to water and visualised every 30 sec using an Olympus Fluoview 1000 confocal microscope with an excitation laser of 543 nm. For paraquat (50 mM), thermal stress (37 ºC, 1 h), sodium azide (0.1 M) and MEC-4(d) studies, animals were incubated in 0.5 mM AO for 2 h in M9. Excess AO was removed by washing the animals five times in M9 before applying the indicated stress or heat shock (for MEC-4(d)). Animals were visualized 4 h later using the confocal microscopy. For propidium iodide staining, worms were incubated in water with 10 μM propidium iodide (Molecular Probes) and visualized using confocal microscopy.

Transmission Electron Microscopy

srp-6(+) or *srp-6(ok319)* animals were exposed to water or M9 for 1, 5 or 15 min and then fixed in 2.5% glutaraldehyde, stained with osmium tetroxide, embedded in agarose and dehydrated through a series of alcohol steps. Animals were sectioned in Spurs resin and visualised by transmission electron microscope, JEOL 1011CX.

RNAi

The *srp-6(RNAi)* plasmid was constructed using the full length SRP-6 cDNA. The *clp-1(RNAi)*, *asp-1(RNAi)*, *asp-3(RNAi)* and *asp-4(RNAi)* plasmids were constructed as described (Syntichaki et al., 2002) and were generously provided by Nektarios Tavernakis. All other RNAi clones were obtained from the MRC geneservice RNAi library (http://www.geneservice.co.uk). *E. coli* HT115 were transformed with the RNAi constructs and fed to animals as described (Kamath et al., 2001).

Volumetric Analysis

For volumetric analysis, young adult *srp-6(+)* or *srp-6(ok319)* animals were placed on a 2% agarose (prepared with water) slide, pre-equilibrated to 25 ºC or 10 ºC (Lamitina et al., 2004). Slide temperature was maintained using a Harvard stage temperature controller. Using a stereomicroscope, animals were visualised under constant magnification for 14 min with images taken every 10 sec. The length and width (averaged from three different regions) were measured using a micrometer and these values were used to approximate the volume of the organism using the equation: $L \times \pi \times r^2$. The relative volume = the volume at the indicted time point/volume at time zero. Eight animals were tested per strain and temperature condition.

Enzymes, Inhibitors and Substrates

CatG, catL, chymotrypsin, thrombin, trypsin, calpain-2 and urokinase-type plasminogen activator were available commercially. Recombinant catK and catV were prepared as described (Bromme et al., 1999; Bromme et al., 1996). The substrate for chymotrypsin and catG was Succinyl-Ala-Ala-Pro-Phe-para-nitroanilide (Succ-AAPF-pNA; Sigma). The cysteine peptidase substrate was $(Z\text{-Phe-Arg})_2$-R110 ($(Z\text{-FR})_2$-R110; Molecular Probes). The calpain-2 substrate was Succinyl-Leu-Leu-Val-Tyr-AMC (Succ-LLVY-AMC; Biomol). PBS reaction buffer (10 mM phosphate buffer, 27 mM KCl, 137 mM NaCl pH 7.4) was used with chymotrypsin and catG. Cathepsin reaction buffer pH 5.5 (50 mM sodium acetate pH 5.5, 4 mM dithiothreitol, 1 mM EDTA) was used with the cysteine peptidases, catK, L and V. The calpain reaction buffer was 50 mM Tris pH 7.5, 150 mM NaCl, 5 mM $CaCl_2$ and 4 mM DTT.

Enzyme Kinetics

As an initial test for inhibitor activity, different peptidases and a 10-25-fold molar excess SRP-6 were incubated for 30 min at 25 °C in the appropriate reaction buffer (Schick et al., 1997). Residual enzyme activity was measured by the addition of substrate. Activity of enzyme in the presence of inhibitor was compared to an uninhibited control.

The second-order rate constant (k_a) for the interaction between SRP-6 and either catL or calpain-2 was determined using the progress curve method (Morrison and Walsh, 1988) under first-order conditions as described (Schick et al., 1998). Human catL and rat recombinant calpain-2 were calibrated by active site titration using E64 as previously described (Schick et al., 1998). The concentration of recombinant SRP-6 was determined by Bradford analysis and thermal stability.

CatL (5 nM) and the substrate $(Z\text{-FR})_2$-R110 (50 μM) were added to different concentrations of SRP-6 (0 nM, 28 nM, 56 nM, 84 nM, 140 nM and 196 nM) and rate of product formation was measured over time using a fluorescent plate reader (Molecular Devices). Assuming an irreversible reaction, the first-order rate constants (k_{obs}) were calculated by a

nonlinear regression fit to each curve using the equation described (Schick et al., 1998). The slope of the line of k_{obs} versus [SRP-6] yields a second-order rate constant, which was corrected for the substrate concentration and the K_m of catL for the substrate (K_m = 2 μM). All data were fit using GraphPad Prism 2.0a for Power Macintosh. For the second reaction, calpain-2 (90 nM) and the substrate Succ-LLVY-AMC (0.5 mM) were added to SRP-6 at 0 nM, 900 nM, 1200 nM, 1500 nM, 2240 nM and 2800 nM. The K_m of calpain-2 for Succ-LLVY-AMC was 5 mM.

Stoichiometry of Inhibition (SI)

The SI for each SRP-6-peptidase interaction was determined as described (Schick et al., 1997; Schick et al., 1998). Briefly, recombinant SRP-6 was incubated at 25ºC for 30 min with 20 nM human catL or for 15 min with 100 nM rat calpain-2. Upon addition of substrate, residual enzyme activity was measured by monitoring the change in relative fluorescence units (RFU). The SI was determined by plotting the ratio of the velocity of inhibited enzyme (v_i) to the velocity of the uninhibited control (v_0) (fractional activity) versus the ratio of inhibitor to enzyme ($[I]_0/[E]_0$), where $[I]_0$ and $[E]_0$ are the serpin and peptidase concentration at time 0, respectively, and extrapolating to zero activity.

Complex Formation

SRP-6 was expressed and labelled using an *in vitro* transcription-translation system (30 ºC for 1 h), 25 μg of plasmid DNA and ^{35}S-methionine according to the manufacturers protocol (Roche). ^{35}S-SRP-6 was incubated with catL (0.5 μg) or calpain-2 (1 μg ± 5mM Ca^{2+}) for 5 or 30 min, respectively, at 25ºC in the appropriate reaction buffer. The reaction products were separated by SDS-PAGE. The gels were dried and examined by autoradiography.

Cleavage Site Determination

Recombinant SRP-6 (4 μg) was mixed with catL (1 μg) or calapin-2 (0.25 μg) and incubated for 2 or 1 min, respectively, at 25 ˚C. The reaction products were analyzed by MADLI-MS as described (Askew et al., 2001).

Table S1. Inhibitory Profile of SRP-6

Peptidase (final concentration)	SRP-6 (nM)	Ratio ($[I]_0/[E]_0$)	Inhibition (%)	Substrate (final concentration)
Chymotrypsin (50 nM)	500	10	0	Succ-AAPF-pNA (1 mM)
Cathepsin G (50 nM)	500	10	0	Succ-AAPF-pNA (1 mM)
Thrombin (50 nM)	500	10	0	$(Z\text{-}PR)_2$- R110 (5 μM)
Kallikrein (50 nM)	500	10	0	$(Z\text{-}FR)_2$-R110 (5 μM)
Plasmin (50 nM)	500	10	0	VLK-pNA (0.1 mM)
Trypsin (50 nM)	500	10	0	EGR-pNA (0.5 mM)
u-PA (50 nM)	500	10	0	EGR-pNA (0.5 mM)
t-PA (50 nM)	500	10	0	EGR-pNA (0.5 mM)
Papain (20 nM)	500	25	99	MeO-Succ-AAPV-pNA (0.5 mM)
Cathepsin K (20 nM)	500	25	94	$(Z\text{-}FR)_2$-R110 (5 μM)
Cathepsin L (20 nM)	500	25	99	$(Z\text{-}FR)_2$-R110 (5 μM)
Cathepsin V (20 nM)	500	25	99	$(Z\text{-}FR)_2$-R110 (5 μM)
Cathepsin H (20 nM)	500	25	0	$(Z\text{-}FR)_2$-R110 (5 μM)
Cathepsin B (20 nM)	500	25	10	$(Z\text{-}FR)_2$-R110 (5 μM)
Calpain-1 (100 nM)	500	5	0	Succ-LLVY-AMC (100 μM)
Calpain-2 (100 nM)	500	5	96	Succ-LLVY-AMC (100 μM)

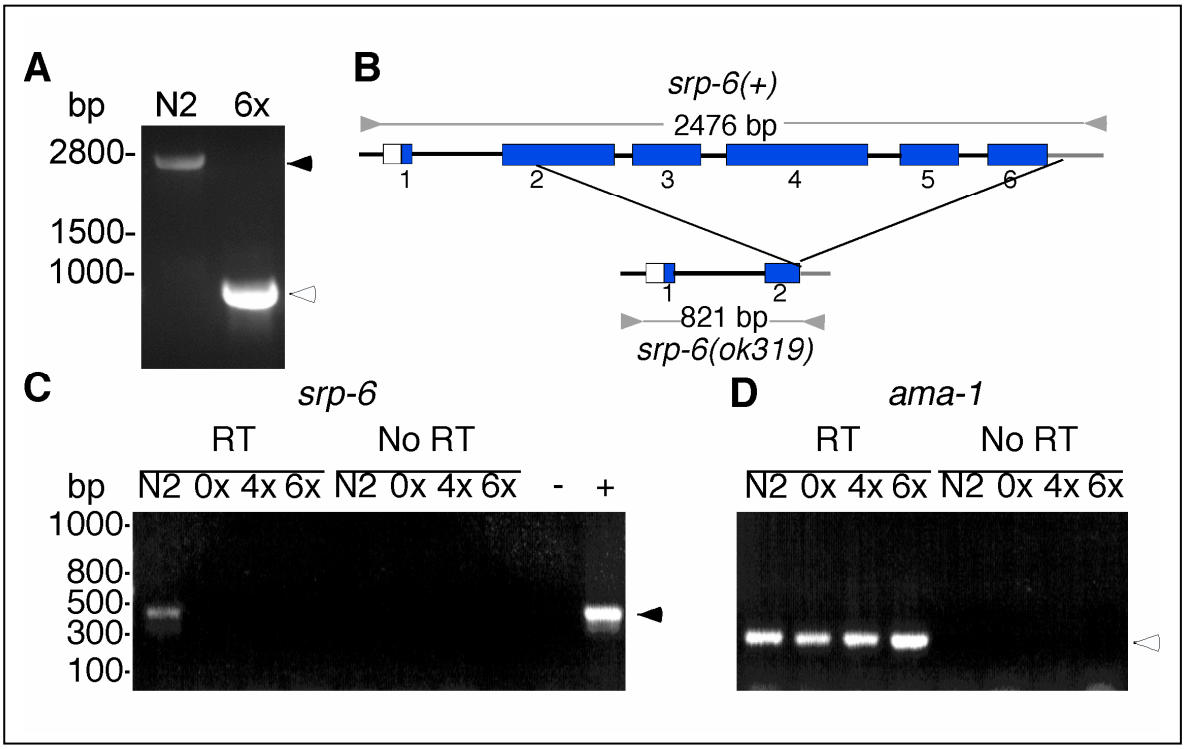

Figure S1. *srp-6(ok319)* Genotype

(A) Amplification of the interstitial deletion in *srp-6(ok319)* animals. N2 wild-type (lane 1) and *srp-6(ok319)* (lane 2) DNAs were amplified with oligonucleotide primers flanking exon 1 and the 3'-UTR (positions of primers are indicated by grey arrowheads in B). Amplicon sizes for wild-type *srp-6* and *srp-6(ok319)* were 2476-bp and 821-bp, respectively.

(B) Map of the deletion within *srp-6(ok319)* animals based on DNA sequencing of the 821-bp deletion fragment. This interstitial deletion eliminates ~85% coding region, including most key structural elements and the reactive site loop.

(C) Absence of SRP-6 mRNA in *srp-6(ok319)* animals. mRNA from N2 wild-type and *srp-6(ok319)* animals (outcrossed 0, 4 or 6 times) was analyzed by reverse transcriptase (RT)-PCR. *srp-6* specific primers amplified a 425-bp fragment from exon 1 to 3. Controls included no RT samples, no DNA (-) and SRP-6 cDNA in pCR4 (+). Black arrowhead indicates position of the SRP-6 specific band.

(D) RNA quality control. The same samples in C were also amplified using *ama-1* (RNA polymerase II) mRNA primers, which yielded a 285-bp band (white arrowhead).

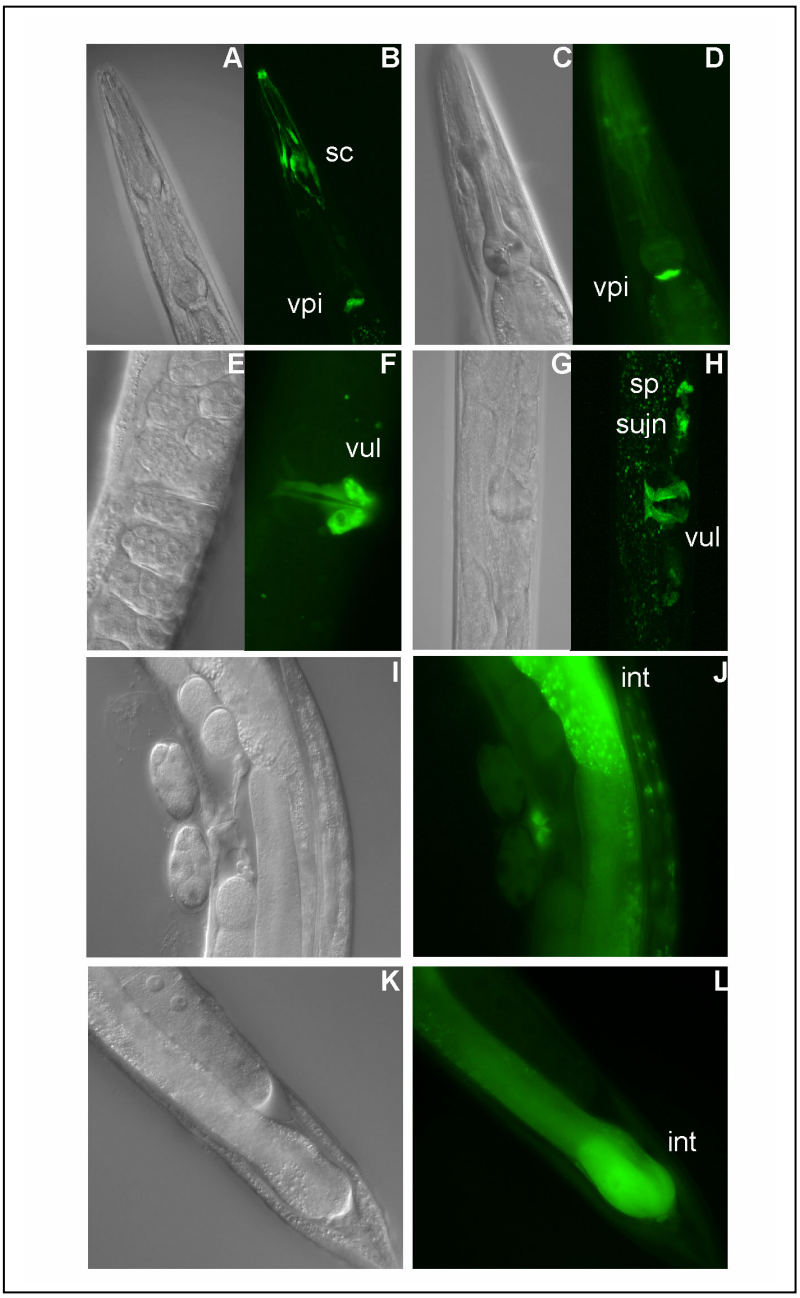

Figure S2. SRP-6 Expression in *C. elegans*
(A-L) *C. elegans* strain VK279 (*srp-6(+);vkEx279[srp-6(ex1-2)::GFP;rol-6]*) expressing a *srp-6::GFP* fusion was visualized using either an Olympus Fluoview 1000 confocal microscope with an excitation laser of 488 nm (B, H) or a Zeiss Axioskop II with an excitation filter of 492 nm and emission filter of 530 nm (D, F, J, L), along with their corresponding DIC images (A, C, E, G, I, K). SRP-6::GFP was expressed in the socket cells (sc; B), the pharyngeal-intestinal valve (vpi; B, D), vulval hypoderm (vul; F, H), the spermatheca (sp) and spermathecal-uterine junction (sujn; H) and the intestine (J, L). Corresponding expression was seen in the *srp-6::lacZ* fusions (not shown).

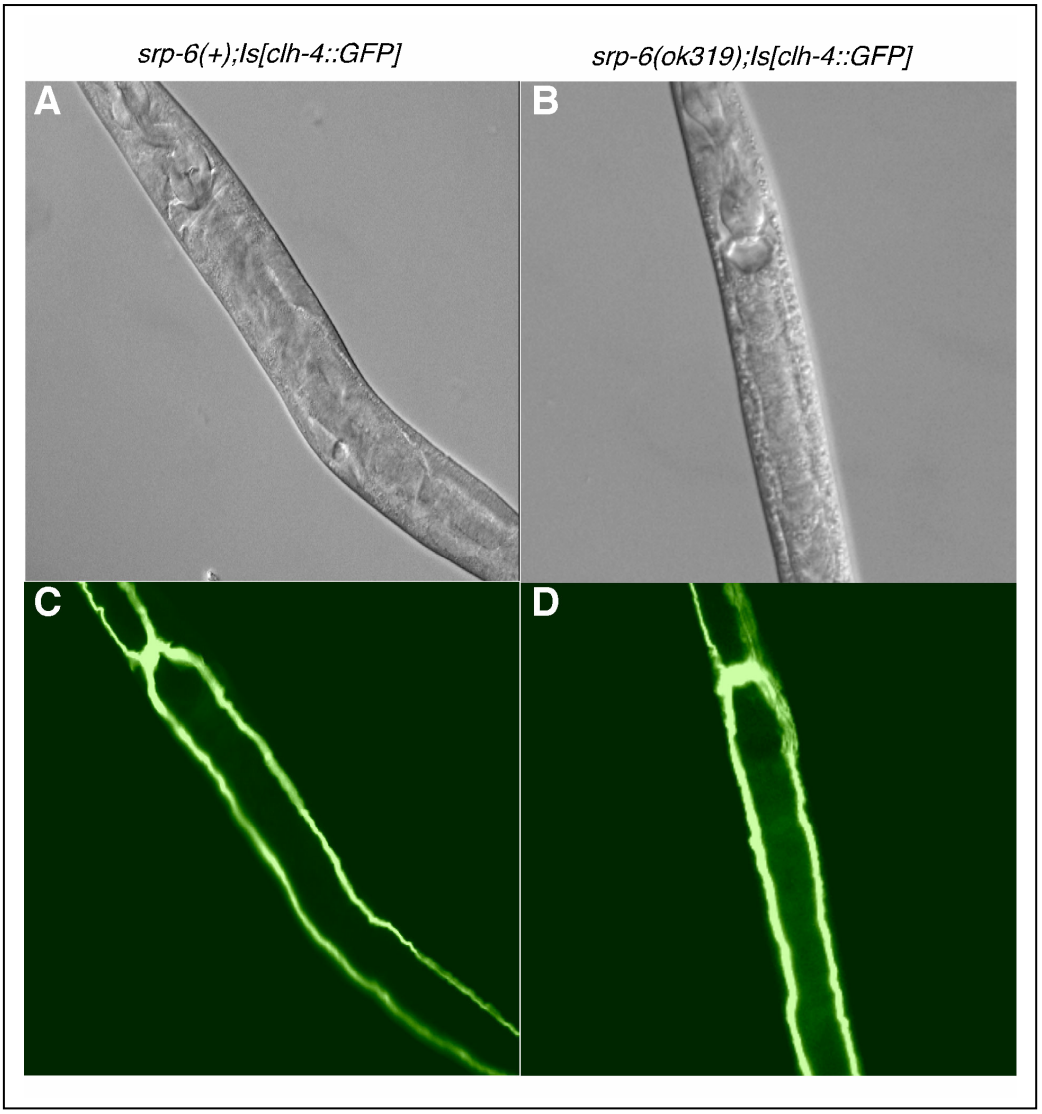

Figure S3. The Excretory Cell in *srp-6(ok319)* Animals
(A-D) *srp-6(+)* (A, B) and *srp-6(ok319)* (C, D) expressing *clh-4::GFP* transcriptional fusions were imaged using a Zeiss Axioskop II with an excitation filter of 492 nm and emission filter of 530 nm. The excretory canal is pseudocolored green (B, D).

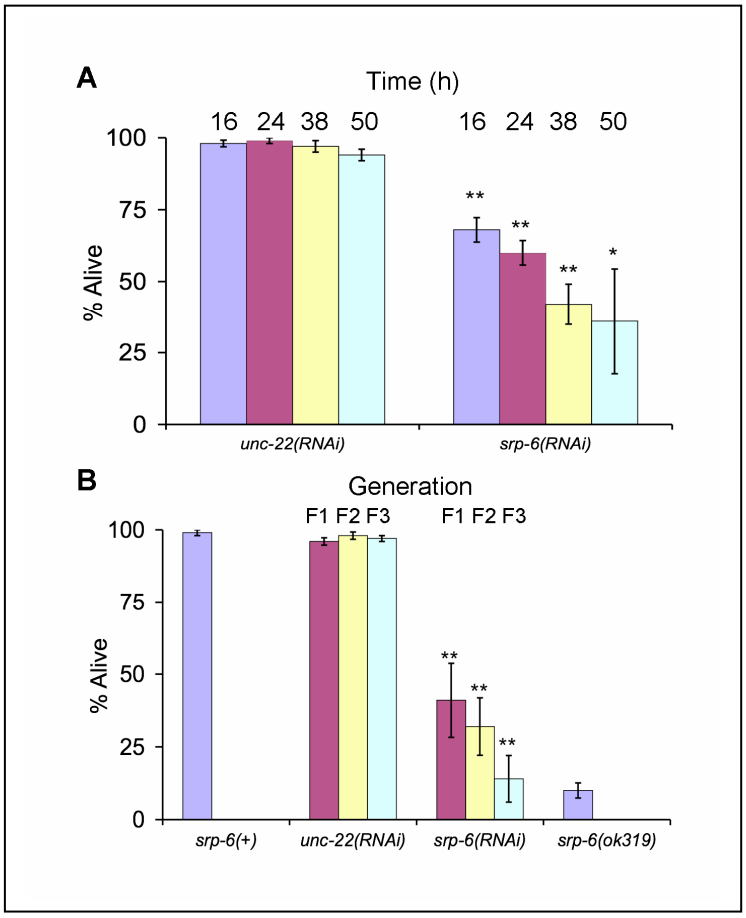

Figure S4. *srp-6(RNAi)* Phenocopied Osl

(A) Mean survival of young adult *srp-6(+)* animals exposed to *srp-6(RNAi)* or *unc-22(RNAi)* by feeding bacteria expressing the respective double-stranded RNAs. Animals fed on bacteria for the indicated time were assayed for survival by exposure to water at 25 ˚C for 30 min. Differences in survival between *srp-6(RNAi)* and control *unc-22(RNAi)* at each feeding time point were compared. Asterisks indicate that the survival between groups was significantly different ($n \approx 300$ animals/group, single and double asterisks indicate $P < 0.05$ and < 0.01, respectively).

(B) Survival of successive generations (F1-F3) of *srp-6(+)* animals exposed continuously to *srp-6(RNAi)* or *unc-22(RNAi)* by feeding. Young adults from each generation were assayed for survival as above ($n \approx 300$ animals/group, single and double asterisks indicate $P < 0.05$ and < 0.01, respectively). The survival of *srp-6(+)* and *srp-6(ok319)* were assayed in parallel and served as controls for the killing assays.

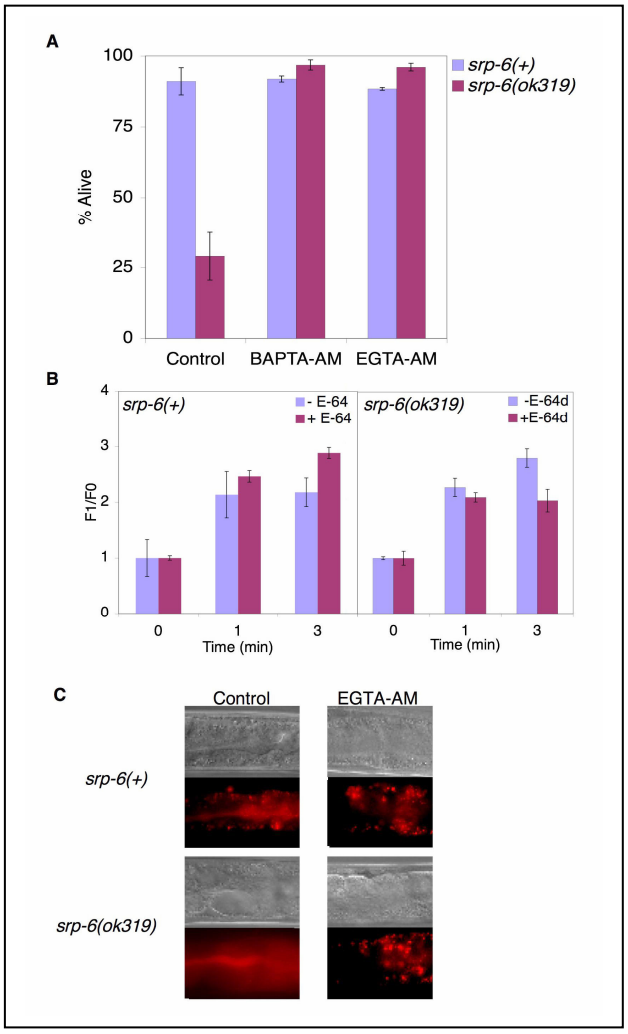

Figure S5. Effects Intracellular Calcium on the Osl Phenotype

(A) Chelation of intracellular calcium prevented Osl. Young adult *srp-6(+)* (blue) and *srp-6(ok319)* (red) animals were incubated in 1% DMSO (control), 100 µM BAPTA-AM in 1% DMSO or 100 µM EGTA-AM in 1% DMSO. Worms were assayed for survival by exposure to water at 25 ˚C for 30 min. Error bars depict the standard deviation from the mean ($n \geq 200$ animals/group).

(B) Cysteine peptidase inhibition did not block the rise in $[Ca^{2+}]_i$ induced by hypotonic shock. Changes in $[Ca^{2+}]_i$ in young adult *srp-6(+)* and *srp-6(ok319)* animals were determined using fluorescence microscopy to measure intestinal cell cytoplasmic fluorescence of the calcium indicator, Fluo-4 AM at the indicated time points. Error bars depict the standard error from the mean ($n \geq 10$ animals).

(C) Chelation of intracellular calcium prevents lysosomal rupture. Adult *srp-6(+)* or *srp-6(ok319)* animals were labelled with AO and then incubated in 1% DMSO (control) or 100 µM EGTA-AM in 1% DMSO before exposure to water at 25 ˚C for 30 min. Worms were visualized by DIC and fluorescence microscopy with excitation and emission wavelengths of 572 nm and 630 nm, respectively, using a Zeiss Axioskop II Mot. Fluorescence images are pseudocolored red. *srp-6(ok319)* control animals lost the punctate lysosomal staining after exposure to water giving diffuse cytoplasmic red staining, but retained their lysosomal integrity in the presence of EGTA-AM.

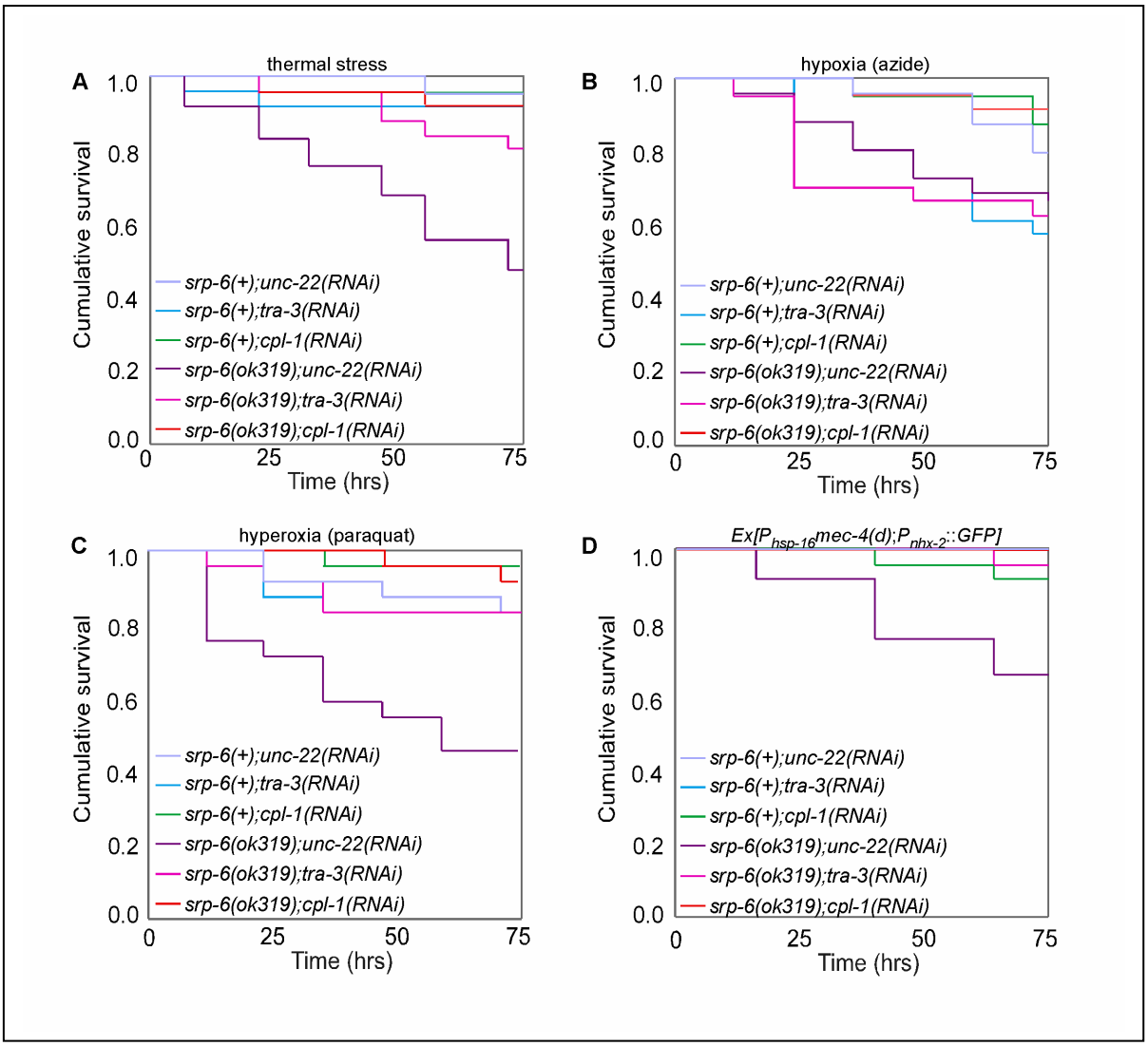

Figure S6. Calpain and Lysosomal Cysteine Peptidase RNAi Suppressed Several Inducers of Necrotic Cell Death in *srp-6(ok319)* Animals

(A-D) Representative Kaplan-Meier curves comparing the survival of adult *srp-6(+)* and *srp-6(ok319)* animals (both strains in (D) also contained the P_{hsp-16}*mec-4(d)* transgene) fed for one generation with *unc-22(RNAi)*, *tra-3(RNAi)* or *cpl-1(RNAi)* inducing bacteria and subsequently exposed to (A) heat shock (1 h at 37 ºC; n = 25), (B) hypoxia (0.1 M sodium azide in M9 for 1 h at 25 ºC; n = 25), (C) hyperoxia (8 mM paraquat in M9 for 2 h at 25 ºC; n = 25) or (D) transgene activation of the necrotic cell death inducer, P_{hsp-16}*mec-4(d)* (induction for 16 h at 30 ºC). Statistical significance was assessed using the log-rank test. In all cases, the survival of *srp-6(ok319);unc-22(RNAi)* animals was statistically less than that of *srp-6(+);unc-22(RNAi)* animals ($P < 0.01$). However, *srp-6(ok319);tra-3(RNAi)* and *srp-6(ok319);cpl-1(RNAi)* were not significantly different from *srp-6(+);tra-3(RNAi)* and *srp-6(+);cpl-1(RNAi,* indicating that *tra-3(RNAi)* and *cpl-1(RNAi)* protected against these necrotic cell death stimuli as they did with Osl. Note, *tra-3(RNAi)* appeared to sensitize *srp-6(+)* animals to sodium azide.

Supplemental References

Askew, Y.S., Pak, S.C., Luke, C.J., Askew, D.J., Cataltepe, S., Mills, D.R., Kato, H., Lehoczky, J., Dewar, K., Birren, B.*, et al.* (2001). SERPINB12 is a novel member of the human ov-serpin family that is widely expressed and inhibits trypsin-like serine proteinases. J Biol Chem *276*, 49320-49330.

Bromme, D., Li, Z., Barnes, M., and Mehler, E. (1999). Human cathepsin V functional expression, tissue distribution, electrostatic surface potential, enzymatic characterization, and chromosomal localization. Biochemistry *38*, 2377-2385.

Bromme, D., Okamoto, K., Wang, B.B., and Biroc, S. (1996). Human cathepsin O2, a matrix protein-degrading cysteine protease expressed in osteoclasts. Functional expression of human cathepsin O2 in Spodoptera frugiperda and characterization of the enzyme. J Biol Chem *271*, 2126-2132.

Driscoll, M., and Chalfie, M. (1991). The mec-4 gene is a member of a family of Caenorhabditis elegans genes that can mutate to induce neuronal degeneration. Nature *349*, 588-593.

Espelt, M.V., Estevez, A.Y., Yin, X., and Strange, K. (2005). Oscillatory Ca2+ signaling in the isolated Caenorhabditis elegans intestine: role of the inositol-1,4,5-trisphosphate receptor and phospholipases C beta and gamma. The Journal of general physiology *126*, 379-392.

Hermann, G.J., Schroeder, L.K., Hieb, C.A., Kershner, A.M., Rabbitts, B.M., Fonarev, P., Grant, B.D., and Priess, J.R. (2005). Genetic analysis of lysosomal trafficking in Caenorhabditis elegans. Mol Biol Cell *16*, 3273-3288.

Kamath, R.S., Martinez-Campos, M., Zipperlen, P., Fraser, A.G., and Ahringer, J. (2001). Effectiveness of specific RNA-mediated interference through ingested double-stranded RNA in Caenorhabditis elegans. Genome Biol *2*, 2.1-2.10.

Lamitina, S.T., Morrison, R., Moeckel, G.W., and Strange, K. (2004). Adaptation of the nematode Caenorhabditis elegans to extreme osmotic stress. Am J Physiol Cell Physiol *286*, C785-C791.

Morrison, J.F., and Walsh, C.T. (1988). The behavior and significance of slow-binding enzyme inhibitors. Adv Enzymol Relat Areas Mol Biol *61*, 201-301.

Nehrke, K. (2003). A reduction in intestinal cell pHi due to loss of the Caenorhabditis elegans Na+/H+ exchanger NHX-2 increases life span. J Biol Chem *278*, 44657-44566.

Schick, C., Kamachi, Y., Bartuski, A.J., Cataltepe, S., Schechter, N.M., Pemberton, P.A., and Silverman, G.A. (1997). Squamous cell carcinoma antigen 2: a novel serpin that inhibits the chymotrypsin-like proteinases cathepsin G and mast cell chymase. J Biol Chem *272*, 1849-1855.

Schick, C., Pemberton, P.A., Shi, G.-P., Kamachi, Y., Cataltepe, S., Bartuski, A.J., Gornstein, E.R., Bromme, D., Chapman, H.A., and Silverman, G.A. (1998). Cross-class inhibition of the cysteine proteinases cathepsins K, L, and S by the serpin squamous cell carcinoma antigen 1: A kinetic analysis. Biochemistry *37*, 5258-5266.

Syntichaki, P., Xu, K., Driscoll, M., and Tavernarakis, N. (2002). Specific aspartyl and calpain proteases are required for neurodegeneration in C. elegans. Nature *419*, 939-944.